Plant, Cell & Environment

Plant, Cell and Environment (2009) **32**, 1695–1709 doi: 10.1111/j.1365-3040.2009.02029.x

A hierarchical Bayesian approach for estimation of photosynthetic parameters of C_3 plants

LISA D. PATRICK[1,2], KIONA OGLE[2] & DAVID T. TISSUE[1,3]

[1]Department of Biological Sciences, Texas Tech University, Lubbock, TX 79409, USA, [2]Departments of Botany and Statistics, University of Wyoming, Laramie, WY 82071, USA and [3]Centre for Plants and the Environment, University of Western Sydney, Richmond, NSW 2753, Australia

ABSTRACT

We describe a hierarchical Bayesian (HB) approach to fitting the Farquhar *et al.* model of photosynthesis to leaf gas exchange data. We illustrate the utility of this approach for estimating photosynthetic parameters using data from desert shrubs. Unique to the HB method is its ability to simultaneously estimate plant- and species-level parameters, adjust for peaked or non-peaked temperature dependence of parameters, explicitly estimate the 'critical' intracellular [CO_2] marking the transition between ribulose 1·5-bisphosphate carboxylase/oxygenase (Rubisco) and ribulose-1,5-bisphosphate (RuBP) limitations, and use both light response and CO_2 response curve data to better inform parameter estimates. The model successfully predicted observed photosynthesis and yielded estimates of photosynthetic parameters and their uncertainty. The model with peaked temperature responses fit the data best, and inclusion of light response data improved estimates for day respiration (R_d). Species differed in R_{d25} (R_d at 25 °C), maximum rate of electron transport (J_{max25}), a Michaelis–Menten constant (K_{c25}) and a temperature dependence parameter (ΔS). Such differences could potentially reflect differential physiological adaptations to environmental variation. Plants differed in R_{d25}, J_{max25}, mesophyll conductance (g_{m25}) and maximum rate of Rubisco carboxylation (V_{cmax25}). These results suggest that plant- and species-level variation should be accounted for when applying the Farquhar *et al.* model in an inferential or predictive framework.

Key-words: *Artemisia tridentata*; *Dasylirion leiophyllum*; *Larrea tridentata*; *Purshia tridentata*; A–C_i curve; A–Q curve; Farquhar *et al.* model; J_{max}; photosynthesis; V_{cmax}.

INTRODUCTION

Mechanistic photosynthetic models based on phenomenological descriptions of the underlying biochemical reactions have broad applications in the field of plant ecophysiology. These models may be used to determine the impact of varying environmental conditions – including those predicted to be affected by climate change – on the biochemistry of photosynthesis and carbon acquisition at the leaf and plant levels (e.g. Wohlfahrt, Bahn & Cernusca 1999a). Further, mechanistic photosynthetic models are often used to parameterize vegetation components in process models applied at scales ranging from plant canopies (Baldocchi & Harley 1995; dePury & Farquhar 1997) to landscapes (Kimball *et al.* 2000; Williams *et al.* 2001) to continents (Sellers *et al.* 1996; Foley *et al.* 1998; Pitman 2003). As such, photosynthetic parameters associated with leaf-level models provide valuable, mechanistic information for predicting large-scale effects of future climate change on terrestrial ecosystems.

In the most commonly used mechanistic model of C_3 photosynthesis, carbon assimilation is limited by one of three biochemical processes (Farquhar, von Caemmerer & Berry 1980). That is, the rate of photosynthesis is modelled as the minimum of three functions: (1) the saturation of ribulose 1·5-bisphosphate carboxylase/oxygenase (Rubisco) with respect to carboxylation; (2) electron transport limiting the regeneration of ribulose-1,5-bisphosphate (RuBP); and (3) the amount of triose phosphate exported from the chloroplast. Through fitting this 'Farquhar *et al.*' model (Farquhar *et al.* 1980) to photosynthetic gas exchange measurements (e.g. photosynthetic responses to changes in intercellular CO_2 concentrations; A–C_i curve), the following parameters can be estimated: the maximum Rubisco carboxylation rate (V_{cmax}), the maximum rate of electron transport (J_{max}), mitochondrial respiration in the light (R_d) and mesophyll conductance (g_m). Because of the crucial role these parameters play in scaling photosynthesis, it is essential that accurate estimates of these parameters are obtained when fitting mechanistic photosynthetic models to leaf-level empirical data.

Importantly, estimates of the photosynthetic parameters of interest (e.g. V_{cmax}, J_{max}) are sensitive to the statistical estimation methods used to fit the Farquhar *et al.* model (Manter & Kerrigan 2004; Dubois *et al.* 2007; Miao *et al.* 2009). These fitting methods are not yet consistent in the literature and can be categorized into six distinct methods (see Miao *et al.* 2009 for a comprehensive review). The primary difference among these methods is the statistical approach used to determine the transition C_i value (C_{crit}; the

Correspondence: L. D. Patrick. Department of Ecology and Evolutionary Biology, University of Arizona, Tucson, AZ 85721, USA. Fax: +1 520 621 9190; e-mail: Lpatrick@email.arizona.edu

value of C_i used to differentiate between Rubisco and RuBP limitations). In addition to the statistical fitting approach, the accuracy of fitting the Farquhar *et al.* model also relies on: (1) correct representation of the kinetic properties of Rubisco (Sharkey *et al.* 2007), often assumed to be relatively conserved in C_3 plants (von Caemmerer 2000); (2) incorporation of temperature dependencies of parameters, which are described by either exponential or peaked exponential functions (Leuning 1997, 2002; Wohlfahrt *et al.* 1999b; Medlyn, Loustau & Delzon 2002; Kattge & Knorr 2007); (3) incorporation of g_m (Niinemets *et al.* 2009a; Pons *et al.* 2009); and (4) accounting for species- and plant-level differences in both fixed parameters (e.g. kinetic constants), estimated parameters (e.g. V_{cmax}, J_{max}) and temperature dependencies.

Indeed, empirical studies have shown that model parameters do vary by plant and species as a result of genetic or environmental variation. For example, mesophyll conductance (g_m), which partially controls the transfer of CO_2 from the mesophyll intercellular space to the site of carboxylation, has been shown to respond to light and leaf anatomy (Evans & von Caemmerer 1996; Tholen *et al.* 2008; Warren 2008; Loreto, Tsonev & Centritto 2009). This variability is important to recognize, because variation in g_m has been linked to changes in photosynthetic capacity (von Caemmerer & Evans 1991; Lloyd *et al.* 1992; Loreto *et al.* 1992; Niinemets *et al.* 2009b). Rubisco kinetic constants (e.g. K_c, K_o) also change across diverse species and environmental conditions (Tcherkez, Farquhar & Andrews 2006). Paradoxically, while variability in such model parameters has been widely documented, many studies have not yet incorporated intra- and interspecific parameter variability into procedures for fitting the Farquhar *et al.* model. Subsequently, application of this model may incorrectly conclude that significant differences exist in parameter estimates for plants, species or treatments, thereby limiting the accuracy of this popular photosynthetic model.

In light of the need for accurate plant- and species-level estimates of photosynthetic parameters under varying environmental conditions, we describe a statistically rigorous method to estimate C_3 photosynthetic parameters. Specifically, we implemented a hierarchical Bayesian (HB) framework that couples the Farquhar *et al.* model with multiple photosynthetic data sets, allowing estimation of plant- and/or species-level variability of kinetic constants and biochemical parameters. While other gas exchange data (e.g. A–Q; light response curves) are often collected in conjunction with A–C_i curves, these data are rarely incorporated into the fitting procedure, although they may help to inform the biochemical processes regulating photosynthesis (von Caemmerer 2000). Here, we use both A–C_i and A–Q data to simultaneously estimate all photosynthetic parameters, including a C_{crit} value specific to each curve. Another attractive feature of the HB approach is that we can explicitly accommodate the nested sampling design such that the photosynthetic parameters are modelled hierarchically (e.g. curves/plants nested in species).

To illustrate and evaluate the HB approach, we used field data collected from four species of common North American desert shrubs. Desert plants were chosen because their photosynthetic responses differ greatly from temperate forest and agricultural species – which are most commonly studied with respect to parameterizing the Farquhar *et al.* photosynthetic model – based on sensitivity to water limitation and temperature (Ogle & Reynolds 2002). By comparing HB model parameter estimates for desert plants with estimates in the literature from temperate forest and crop plants, we highlight the potential importance of incorporating: (1) flexibility in defining kinetic and biochemical parameter values; (2) plant- and species-specific parameter variability when estimating photosynthetic parameters; and (3) more rigorous statistical methods for analyzing photosynthetic data in the context of mechanistic models such as the Farquhar *et al.* model.

METHODS

Study sites, plants and field measurements

Photosynthetic data for shrub species used in this study were collected at three study sites, each within a distinct North American desert ecosystem. In the Great Basin Desert, the field site was located near the Sierra Nevada Aquatic Research Laboratory (SNARL) of the Valentine Eastern Sierra UC (University of California) Natural Reserve, in eastern California near the city of Mammoth Lakes (37°37′N, 118°50′W, elevation 2100 m). Mean annual precipitation (MAP) is approximately 386 mm, most of which is received between October and March as snow or convective rainstorms. For more detailed SNARL site characteristics, see Gillespie & Loik (2004) and Loik (2007). In the Mojave Desert, data were collected at the Mojave Global Change Facility (MGCF) located on the Nevada Test Site (36°49′N, 115°55′W, elevation 970 m). MAP at the MGCF is about 138 mm, occurring primarily during the winter months (Hunter 1995), with highly episodic summer precipitation and a low relative frequency of large rainfall events. For a more detailed MGCF site description, see Barker *et al.* (2006). In the Chihuahuan Desert, the study site was located in a sotol grassland ecosystem within the Pine Canyon Watershed in Big Bend National Park (BIBE), Texas (29°5′N, 103°10′W, elevation 1526 m). MAP is about 370 mm, with the majority of annual precipitation occurring during the summer months and arriving as monsoonal rains. For a more detailed BIBE site description, see Patrick *et al.* (2007, 2009) and Robertson *et al.* (2009).

At SNARL, measurements were collected on *Artemisia tridentata* (ARTR; Asteraceae, $n = 5$ plants) and *Purshia tridentata* (PUTR; Rosaceae, $n = 5$ plants), two native C_3 woody shrubs in the sagebrush scrub ecosystem. These species are codominant in the ecosystem, representing about 80% of the plant cover (Loik 2007). At MGCF, measurements were made on the native, dominant C_3 evergreen shrub, *Larrea tridentata* (LATR; Zygophyllaceae, $n = 4$ plants). At BIBE, measurements were made on the

dominant C_3 perennial shrub, *Dasylirion leiophyllum* (DALE; Liliaceae, $n = 3$ plants).

During the 2005 growing season (May–August), *A–Q* curves (Supporting Information Fig. S1) were measured on each study plant at each site using a portable photosynthetic system (model Li-6400; Li-Cor, Lincoln, NE, USA). During the 2006 growing season (May–August), both A–C_i and *A–Q* curves were measured on the same study plants as the previous year. A–C_i curves were measured at saturating irradiance (1500 μmol m^{-2} s^{-1}) for 12 CO_2 concentrations in the following order (first to last measurement): 0, 50, 100, 150, 200, 250, 380, 500, 700, 900, 1200 and 1500 μmol mol^{-1}. To ensure steady-state conditions, the plants were allowed to acclimate to ambient CO_2 (380 μmol mol^{-1}) in the gas exchange chamber for approximately 5 min before beginning each A–C_i curve, and then logged. This logged measurement was then compared to the measurement at identical [CO_2] in the middle of the curve sequence to confirm full enzyme activation. It took approximately 45 min to complete a single A–C_i curve. *A–Q* curves were measured at ambient [CO_2] (400 μmol mol^{-1}) for 12 light levels in the following order (first to last): 2000, 1500, 1000, 800, 600, 400, 300, 200, 100, 70, 40 and 0 μmol m^{-2} s^{-1}. The plants were allowed to acclimate to changes in light intensity for approximately 2–3 min before measurements were logged; it took about 35 min to complete an entire *A–Q* curve.

Across all plants and curve types, leaf temperature and relative humidity were recorded and set to ambient values. Average temperature and relative humidity were 26.1 °C and 48.9%, respectively, and ranged from 11.2 to 44.4 °C, and from 7.2 to 94.1%, respectively. All curves were measured from the early morning to the early afternoon when day-time air temperature was near its daily minimum, vapour pressure deficit was relatively low and stomata were responsive to changes in CO_2 and light. All measurements of photosynthesis and stomatal conductance were corrected for leaf area. A total of 17 A–C_i curves and 37 *A–Q* curves were measured across all species, providing 696 observations of photosynthesis.

HB model of photosynthesis

Plant photosynthetic data were analysed within an HB framework (Clark 2005; Clark & Gelfand 2006). This approach has been successfully used to synthesize ecological data (e.g. Clark & LaDeau 2006; Ogle & Barber 2008), and it has proven to be exceptionally useful for making inferences about ecosystem and plant physiological responses (Cable *et al.* 2008, 2009; Ogle *et al.* 2009; Patrick *et al.* 2009). We propose that the HB approach is advantageous for modelling photosynthesis because it can: (1) simultaneously estimate unknown parameters – related to biochemical limitations of photosynthesis – while also accounting for uncertainty in measurements and parameters (Carlin, Clark & Gelfand 2006; Ogle & Barber 2008); (2) accurately estimate common photosynthetic parameters without the need for subjective determination of thresholds for limiting biochemical processes [e.g. it allows us to avoid setting a fixed and potentially arbitrary transition intracellular CO_2 (C_{crit}) value to separately estimate V_{cmax} and J_{max}]; (3) simultaneously incorporate a variety of data types (e.g. A–C_i and *A–Q* curve data) to arrive at parameter estimates and parameter variability; (4) allow for borrowing of strength between curves to help estimate population-level parameters of interest (e.g. species-specific biochemical parameters); and (5) incorporate prior information for biochemical parameters that may not be well informed by the A–C_i and *A–Q* response curve data, but that reflect appropriate levels of uncertainty based on variation in these parameters as reported in the literature. We emphasize that the HB model provides the statistical framework for fitting a process-based model such as the Farquhar *et al.* model to observational data. That is, we do not present modifications to the Farquhar *et al.* model, but describe a rigorous and statistically consistent methodology for confronting such a model with diverse data.

The HB model has three primary components: (1) the observation equation that describes the likelihood of observed photosynthesis data; (2) the process equation that describes the 'true' or mean photosynthetic response, based on the Farquhar *et al.* model of C_3 photosynthesis, as well as process uncertainty associated with random effects; and (3) prior distributions for process model parameters (e.g. species effects) and variance terms. These three parts are combined to generate posterior distributions of all unknown parameters (see Wikle 2003; Clark 2005), including photosynthesis-related parameters and all variance/covariance terms. All probability distributions are parameterized according to Gelman *et al.* (2004). Table 1 includes a list of abbreviations and units for parameters used in the model. The model was run with two different photosynthetic data sets: (1) observations for A–C_i curves only ($n = 207$); and (2) observations from both *A–Q* and A–C_i curves ($n = 696$) to determine if *A–Q* curve data can improve estimates of photosynthetic parameters.

The observation equation

The likelihood of all leaf-level photosynthesis data is based on the likelihood of individual observations of photosynthesis obtained from the Li-6400 (i.e. *Aobs*; μmol m^{-2} s^{-1}). We assumed that the photosynthetic measurements could be described by a normal distribution, such that for observation i ($i = 1, 2, \ldots, N$):

$$Aobs_i \sim \text{Normal}(\bar{A}_i, \tau) \quad (1)$$

where $\bar{A}_i$ is the mean or predicted photosynthesis rate, and τ is the precision (1/variance) parameter that describes the variability in the photosynthetic observation or measurement errors.

The process model

The process model describes the predicted photosynthesis rate ($\bar{A}_i$), which was specified according to the Farquhar

Table 1. List of abbreviations used in the coupled hierarchical Bayesian (HB)–photosynthetic model, their definitions and units

Abbreviation	Definition	Units
Observed data for model input		
Aobs	Rate of CO_2 assimilation measured by the Li-Cor 6400	μmol m^{-2} s^{-1}
Ciobs	Intercellular airspace CO_2 partial pressure measured by the Li-Cor 6400	Pa
Qobs	Photosynthetically active radiation measured by the Li-Cor 6400	μmol m^{-2} s^{-1}
Tobs	Leaf temperature measured by the Li-Cor 6400	°C
Pobs	Pressure measured by the Li-Cor 6400	Pa
HB model parameters associated with process model		
$\bar{A}$	Predicted rate of CO_2 assimilation (see Eqn 1)	μmol m^{-2} s^{-1}
A_c	Rubisco-limited rate of CO_2 assimilation	μmol m^{-2} s^{-1}
A_j	Electron transport limited rate of CO_2 assimilation	μmol m^{-2} s^{-1}
E (E_g, E_m, E_r, E_{kc}, E_{ko}, E_v, E_j)	Activation energy used in Arrhenius temperature function	kJ mol^{-1}
f	Spectral light quality factor	
g_m	Conductance for CO_2 diffusion from intercellular airspace to site of carboxylation	μmol m^{-2} s^{-1} Pa^{-1}
H (H_{gm}, H_v, H_j)	Deactivation factor used in Arrhenius temperature function	kJ mol^{-1}
J	Rate of electron transport	μmol m^{-2} s^{-1}
J_{max} (J_{max25})	Maximal electron transport rate (standardized to 25 °C)	μmol m^{-2} s^{-1}
K_c (K_{c25})	Michaelis–Menten constant for Rubisco for CO_2 (standardized to 25 °C)	Pa
K_o (K_{o25})	Michaelis–Menten constant for Rubisco for O_2 (standardized to 25 °C)	kPa
O	Partial pressure of O_2	Pa
Q_2	Photosynthetically active radiation absorbed by PSII	μmol m^{-2} s^{-1}
R	Universal gas constant (8.314 J K^{-1} mol^{-1})	J K^{-1} mol^{-1}
R_d (R_{d25})	Mitochondrial respiration in the light (standardized to 25 °C)	μmol m^{-2} s^{-1}
ΔS (ΔS_{gm}, ΔS_v, ΔS_j)	Entropy factor used in Arrhenius temperature function	J mol^{-1} K^{-1}
T	Leaf temperature	K
T_{opt}	Optimum temperature	K (°C)
V_{cmax} (V_{cmax25})	Maximum rate of Rubisco carboxylation (standardized to 25 °C)	μmol m^{-2} s^{-1}
α	Fraction of PSII activity in the bundle sheath	
Γ^* (Γ^*_{25})	Chloroplastic CO_2 photocompensation point (standardized to 25 °C)	Pa
θ	Empirical curvature factor	
HB parameters associated with hierarchical priors and hyperpriors		
Y_{25}	Plant-level mean of any parameter (Y) standardized to 25 °C	
μY_{25}	Species-level mean of any parameter (Y) standardized to 25 °C	
$\mu^* Y_{25}$	Population-level mean of any parameter (Y) standardized to 25 °C	
τ	Precision (1/variance) parameter describing observation and measurement error	
τ_{Yplant}	Precision (1/variance) parameter describing plant-to-plant variation within species	
τ_{Yspp}	Precision (1/variance) parameter describing species-to-species variability	

et al. model of C_3 photosynthesis (Farquhar *et al.* 1980). The dependence of potential electron transport rate on absorbed irradiance was specified according to Farquhar & Wong (1984). Triose phosphate limitation was not considered here because this process is expected to rarely limit photosynthesis and is not commonly included in models to estimate photosynthetic parameters (Wohlfahrt *et al.* 1999b; Medlyn *et al.* 2002; Dubois *et al.* 2007). Modifications for mesophyll conductance (g_m) were included using quadratic equations as described by von Caemmerer & Evans (1991), von Caemmerer (2000) and Niinemets *et al.* (2009a). In addition, when values of C_i and internal oxygen concentration (O) were converted from μmol mol^{-1} to Pa, they were also corrected for pressure, because the pressure among measurement sites was different from standard pressure (range: 77.3–97.5 kPa). When both the A–C_i and A–Q data sets were included, the Farquhar *et al.* model was still used to model the expected photosynthetic rate, and thus both data sets simultaneously informed parameters in the photosynthetic model. See Table 2 for a list of model equations and parameters used to describe $\bar{A}_i$ in Eqn 1.

Temperature dependencies of Rubisco's carboxylation and oxygenation rates affect photosynthesis (Bjorkman, Badger & Armond 1980), as do the temperature dependencies of V_{cmax} and J_{max} (von Caemmerer 2000). Thus, temperature dependencies for all parameters (i.e. K_c, K_o, Γ^*, g_m, R_d, V_{cmax} and J_{max}; Table 1) were chosen to follow an Arrhenius function (von Caemmerer 2000; Leuning 2002; Medlyn *et al.* 2002; Kattge & Knorr 2007) standardized to 25 °C. The general form of the Arrhenius function for parameter Y (where $Y = K_c$, K_o, Γ^*, g_m, R_d, V_{cmax} or J_{max}) is:

$$Y = f_1(Y_{25}, E_Y, Tobs_i) = Y_{25} \exp\left[\frac{E_Y(Tobs_i - 298)}{(298 \cdot R \cdot Tobs_i)}\right] \quad (2)$$

where Y_{25} is the parameter at 25 °C, E_Y is the activation energy of Y, *Tobs* is the leaf temperature (K) measured by the Li-6400 and R is the universal gas constant

Table 2. List of equations used in the photosynthesis process model

Eqn no.	Equation
2.1	$\bar{A}_i = A_{c_i}$, if $Ciobs_i < C_{crit}$ $\bar{A}_i = A_{j_i}$, if $Ciobs_i > C_{crit}$
2.2	$A_{c_i} = \frac{-b + \sqrt{b^2 - 4ac}}{2a}$ $a = -\frac{1}{g_{m_i}}$ $b = \frac{(V_{cmax_i} - R_{d_i})}{g_{m_i}} + Ciobs_i + K_{c_i}\left(\frac{1 + O_i}{K_{o_i}}\right)$ $c = R_{d_i}\left[Ciobs_i + K_{c_i}\left(\frac{1 + O_i}{K_{o_i}}\right)\right] - V_{cmax_i}(Ciobs_i - \Gamma_i^*)$
2.3	$A_{j_i} = \frac{-b + \sqrt{b^2 - 4ac}}{2a}$ $a = -\frac{1}{g_{m_i}}$ $b = \frac{\frac{J_i}{4} - R_{d_i}}{g_{m_i}} + Ciobs_i + 2\Gamma_i^*$ $c = R_{d_i}(Ciobs_i + 2\Gamma_i^*) - \frac{J_i}{4}(Ciobs_i - \Gamma_i^*)$
2.4	$J_i = \frac{Q_{2i} + J_{max_i} - \sqrt{(Q_{2i} + J_{max_i})^2 - 4\theta Q_{2i} J_{max_i}}}{2\theta}$ where $\theta = 0.7$ (Evans 1989)
2.5	$Q_{2i} = Qobs_i \cdot \alpha(1 - f)/2$, where $\alpha = 0.85$ (von Caemmerer 2000) and $f = 0.15$ (Evans 1987)

All equations are from Farquhar *et al.* (1980), Farquhar & Wong (1984) and von Caemmerer (2000). See Table 1 for abbreviations, definitions and units.

(8.314 J mol^{-1} K^{-1}). To include plant-level variation in the g_m, R_d, V_{cmax} and J_{max} parameters at 25 °C (i.e. the Y_{25}s), these parameters were allowed to vary by curve (or plant). To account for potential species-level differences in temperature dependencies, the activation energies associated with the g_m, R_d, V_{cmax} and J_{max} parameters (E_m, E_r, E_v and E_j, respectively) were allowed to vary by species, such that for observation i, plant p and species s:

$$\begin{aligned} g_{m_i} &= f_1(g_{m25p}, E_{m_{s(p)}}, Tobs_i) \\ R_{d_i} &= f_1(R_{d25p}, E_{r_{s(p)}}, Tobs_i) \\ V_{cmax_i} &= f_1(V_{cmax_{25p}}, E_{v_{s(p)}}, Tobs_i) \\ J_{max_i} &= f_1(J_{max_{25p}}, E_{j_{s(p)}}, Tobs_i) \end{aligned} \quad (3)$$

The notation $s(p)$ is read as 's of p', which represents the species identity associated with each plant (i.e. plant is 'nested' in species). Because the Rubisco kinetic properties at 25 °C (Γ^*_{25}, K_{c25} and K_{o25}) and their associated activation energies (E_g, E_{kc}, E_{ko}) have only been shown to vary by species (von Caemmerer 2000) and are generally not well informed by A–C_i or A–Q data, we assume that these parameters vary at the species level such that:

$$\begin{aligned} \Gamma^*_i &= f_1(\Gamma^*_{25s(p)}, E_{g_{s(p)}}, Tobs_i) \\ K_{c_i} &= f_1(K_{c25s(p)}, E_{kc_{s(p)}}, Tobs_i) \\ K_{o_i} &= f_1(K_{o25s(p)}, E_{ko_{s(p)}}, Tobs_i) \end{aligned} \quad (4)$$

While Eqns 2 and 3 were used for analyses of both data sets, it was also recognized that temperature response functions for g_m, V_{cmax} and J_{max} are commonly modelled (von Caemmerer 2000; Leuning 2002; Medlyn *et al.* 2002; Kattge & Knorr 2007) using the peaked Arrhenius function (Johnson, Eyring & Williams 1942). As such, we also ran the model using the combined A–C_i and A–Q data set with the peaked Arrhenius functions to determine if model fit and parameter estimation were improved by incorporating this more flexible temperature response compared to the non-peaked function in Eqn 2. For this analysis, f_1 in Eqn 2 was replaced with:

$$\begin{aligned} Y &= f_2(Y_{25}, E_Y, Tobs_i, \Delta S_Y, H_Y) \\ &= Y_{25} \exp\left[\frac{E_Y(Tobs_i - 298)}{298 \cdot R \cdot Tobs_i}\right] \frac{1 + \exp\left(\frac{298\Delta S_Y - H_Y}{298R}\right)}{1 + \exp\left(\frac{Tobs_i \Delta S_Y - H_Y}{R \cdot Tobs_i}\right)} \end{aligned} \quad (5)$$

where E_Y is the activation energy, H_Y is the deactivation energy describing the rate of decrease for temperatures above the optimum temperature and ΔS_Y is an entropy factor. Once again, g_{m25}, V_{cmax25} and J_{max25} parameters were allowed to vary by plant, and because species-level variation has been observed in the temperature response parameters (i.e. E, H, ΔS) (Kattge & Knorr 2007), the associated parameters for g_m (E_m, ΔS_{gm}, H_{gm}), V_{cmax} (E_v, ΔS_v, H_v) and J_{max} (E_j, ΔS_j, H_j) also were allowed to vary between species, such that:

$$\begin{aligned} g_{m_i} &= f_2\left(g_{m25p}, E_{m_{s(p)}}, \Delta S_{m_{s(p)}}, H_{m_{s(p)}}, Tobs_i\right) \\ V_{cmax_i} &= f_2\left(V_{cmax25p}, E_{v_{s(p)}}, \Delta S_{v_{s(p)}}, H_{v_{s(p)}}, Tobs_i\right) \\ J_{max_i} &= f_2\left(J_{max25p}, E_{j_{s(p)}}, \Delta S_{j_{s(p)}}, H_{j_{s(p)}}, Tobs_i\right) \end{aligned} \quad (6)$$

The prior model

The final stage in the HB modelling approach was the specification of the priors for the unknown parameters. Because many model parameters varied on a plant and/or species level, nested, hierarchical priors were chosen. The ability to have nested priors is another major advantage of the HB approach because it allows parameters within a given level (e.g. across plants within species or across species) to inform or 'borrow strength' from each other (Carlin *et al.* 2006). Moreover, the nesting of plants within species within an overall population of desert shrubs describes a natural hierarchy that reflects the sampling design. Thus, under this framework, plant-level parameters – which are directly related to individual curve data – are assumed to be nested within species, such that for any plant-level parameter at 25 °C ($Y_{25} = g_{m25}$, R_{d25}, V_{cmax25} and J_{max25}):

$$Y_{25p} \sim \text{Normal}\left(\mu Y_{25s(p)}, \tau_{Yplant}\right) \quad (7)$$

where $\mu Y_{25s(p)}$ is the species-level mean, and τ_{Yplant} is the precision (1/variance) parameter that describes plant-to-plant variability within a species. The species-level parameters were then assumed to be nested within an overall population, such that:

$$\mu Y_{25s} \sim \text{Normal}\left(\mu^* Y_{25}, \tau_{Yspp}\right) \quad (8)$$

where $\mu^* Y_{25}$ is the population-level mean, and τ_{Yspp} is the precision parameter that describes species-to-species variability within the desert shrubs studied here. Standard, independent and relatively non-informative (diffuse) priors were employed for the population-level mean parameters (the $\mu^* Y_{25}$); that is, we used normal densities with large variances (small precisions). Folded-Cauchy (i.e. a Student's t-distribution with one degree of freedom) densities were assigned as priors for all standard deviations ($\sigma = 1/\sqrt{\tau}$, where τ is the precision parameter of interest) as suggested by Gelman (2006). Another advantage of the HB framework is that we were able to incorporate informative priors for the Michaelis–Menten parameters (K_c and K_o), CO_2 compensation point (Γ^*) and the Arrhenius temperature function parameters (E, ΔS, H); that is, we assigned normal distributions centred on values reported in the literature (von Caemmerer 2000) and used small precisions based on coefficients of variation (CV = standard deviation/mean) around 15% (Supporting Information Table S1).

Finally, another advantage of this HB approach is that we were able to specify which parameters should be informed by which data set. For example, we do not expect the A–Q data to contain sufficient information about V_{cmax} because the data were collected under ambient CO_2, and C_i was approximately constant. Thus, within the HB model code (see WinBUGS implementation below), we employed the 'cut' function to sever the feedback between, for example, the A–Q curve data and V_{cmax}. This resulted in posterior distributions for parameters describing V_{cmax} that were solely informed by the A–C_i data, but the uncertainty in the V_{cmax} values was propagated to the predicted photosynthetic values associated with the A–Q data. Using this approach, we assumed that K_c, K_o, Γ^*, g_m, V_{cmax} and J_{max} were solely informed by the A–C_i data, and R_d, C_{crit} and temperature dependence parameters were informed by both data sets (i.e. did not use the cut function with these parameters). Although A–C_i curve data generally do not provide sufficient data on R_d (i.e. all *Aobs* measurements were made under constant, high light), we still allow the A–C_i data to inform R_d because many studies may only measure A–C_i curves in an effort to estimate photosynthetic parameters, including R_d.

The HB model defined by Eqns 1–8 was implemented in the Bayesian statistical software package WinBUGS (Lunn *et al.* 2000). WinBUGS code for the HB model has been provided as supplementary material. Three parallel Markov chain Monte Carlo (MCMC) chains were run for 30 000 iterations each, and the BGR diagnostic tool was used to evaluate convergence of the chains to the posterior distribution (Brooks & Gelman 1998; Gelman 2004a). The burn-in samples (first 4000) were discarded, and the remaining samples (after convergence) were thinned every 20th iteration, yielding an independent sample of 3000 values for each parameter from the joint posterior distribution (Gelman 2004b; Gamerman & Hedibert 2006). Model goodness-of-fit was evaluated by using Eqn 1 to generate replicated data for the observed values ($Aobs_i$) (Gelman *et al.* 2004), yielding posterior predictive distributions for each observation. If the model perfectly predicted the data, all observed-versus-predicted (posterior means for replicated data) points would lie exactly on the 1:1 line. We compared models (e.g. A–C_i data model with non-peaked temperature functions versus A–C_i data model with peaked temperature functions) by computing the posterior predictive loss (D) for each model (Gelfand & Ghosh 1998). D is a model comparison statistic that accounts for model predictive ability ('goodness-of-fit') while penalizing for model complexity, and the model with the lower D value is preferred.

Table 3. r^2 Values for observed versus predicted photosynthesis, posterior predictive loss (D) and estimates of the uncertainty in the D values (i.e. approximate estimates of the 2.5th and 97.5th percentiles) obtained from the hierarchical Bayesian (HB) model using A–C_i data only and combined A–C_i and A–Q data with either non-peaked or peaked temperature response functions for photosynthetic parameters

Data/model combination	r^2	D	2.5%	97.5%
A–C_i only (non-peaked temp.)	0.99	204.7	157.4	265.7
A–C_i only (peaked temp.)	0.99	199.3	150.3	261.4
A–C_i and A–Q (non-peaked temp.)	0.76	31 960	22 820	41 250
A–C_i and A–Q (peaked temp.)	0.87	22 150	13 510	32 750

Note that comparison of the D values is only relevant within a given data set.

RESULTS

Model goodness-of-fit and model comparison

The coupled HB–photosynthetic model fit the data well for A–C_i data only and for the combined A–C_i and A–Q data using both non-peaked and peaked temperature functions (Table 3). For example, points in the plots of observed-versus-predicted photosynthesis fell tightly along the 1:1 line (data not shown). When comparing among models (for a particular data set or data set combination), models that incorporated peaked temperature responses had lower D values compared to models that used non-peaked temperature functions (Table 3). Thus, the results reported below, unless otherwise specified, are from models that employed peaked temperature functions for photosynthetic parameters of interest (g_m, R_d, V_{cmax} and J_{max}).

Utility of *A–Q* data for estimates of biochemical parameters

While the model goodness-of-fit results were not statistically different for both A–C_i data only, and A–C_i and A–Q data combined (Table 3), the addition of A–Q data greatly improved estimation of R_{d25}. Using both data sets, there was a high frequency of positive posterior mean estimates of R_{d25}, while in the model that used only A–C_i data, the lower credible intervals and the posterior means for R_{d25} were often negative (Fig. 1). While we did not estimate R_{d25} using only A–Q data in this study, we expect that our model estimates for A–C_i and A–Q data combined would be similar to A–Q only estimates given that A–C_i data collected here were not able to directly inform R_{d25} because of measurement at high light. The inclusion of A–Q data did not improve estimates of V_{cmax25} or J_{max25}, but this is expected because the A–Q data were not allowed to inform these parameters. Importantly, the ability of A–Q data to inform biochemical parameters other than R_{d25} was limited by our A–Q measurements at ambient [CO_2]. By measuring A–Q curves at above or saturating [CO_2], A–Q data could be used to inform additional biochemical parameters of interest (e.g. J_{max25}). However, because both data sets did inform a subset of parameters, the inclusion of A–Q data had a slight impact on parameter uncertainty such that the posterior estimates for V_{cmax25} or J_{max25} varied more between plant/species and their credible intervals were smaller when using only A–C_i data (Fig. 2; Supporting Information Fig. S2). The use of A–Q data produced more variability in posterior mean estimates and slightly wider posterior credible intervals for C_{crit}, but the range of C_{crit} values was similar using either data set (Fig. 2; Supporting Information Fig. S2).

Parameters poorly informed by photosynthetic data

While the HB model provided an updated estimate of the Michaelis–Menten constant of Rubisco for O_2 (K_{o25}) that was informed by A–C_i data, this was not the case for all energy of activation parameters (E_{kc}, E_{ko}, E_g, E_m, E_r, E_v, E_j) and the peaked temperature parameters (H_{gm}, H_v, H_j). That is, the posterior means for the species-level E and H parameters were very similar to the means specified by their informative prior distributions (Supporting Information Tables S1 & S2). This indicates that these parameters were poorly informed by the photosynthetic data used (Table 4), or the data are in close agreement with the priors. The first explanation is more likely because these parameters became less identifiable under less informative priors.

Parameters well informed by photosynthetic data

The HB model produced posteriors for curve-specific C_{crit} values (used to differentiate between Rubisco- and

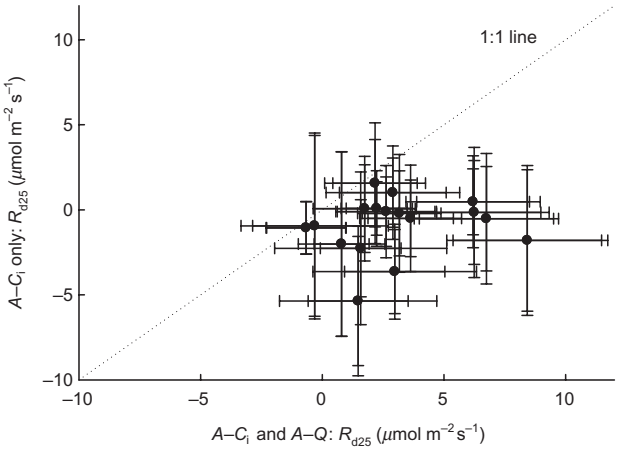

Figure 1. Posterior mean estimates and 95% credible intervals for the plant-level mitochondrial respiration rate standardized to 25 °C (R_{d25}) from the peaked temperature model using only A–C_i data compared to estimates using both A–C_i and A–Q data. R_{d25} estimates from the combined data sets are greater than zero, while many of the R_{d25} estimates for the 'A–C_i only' data are negative.

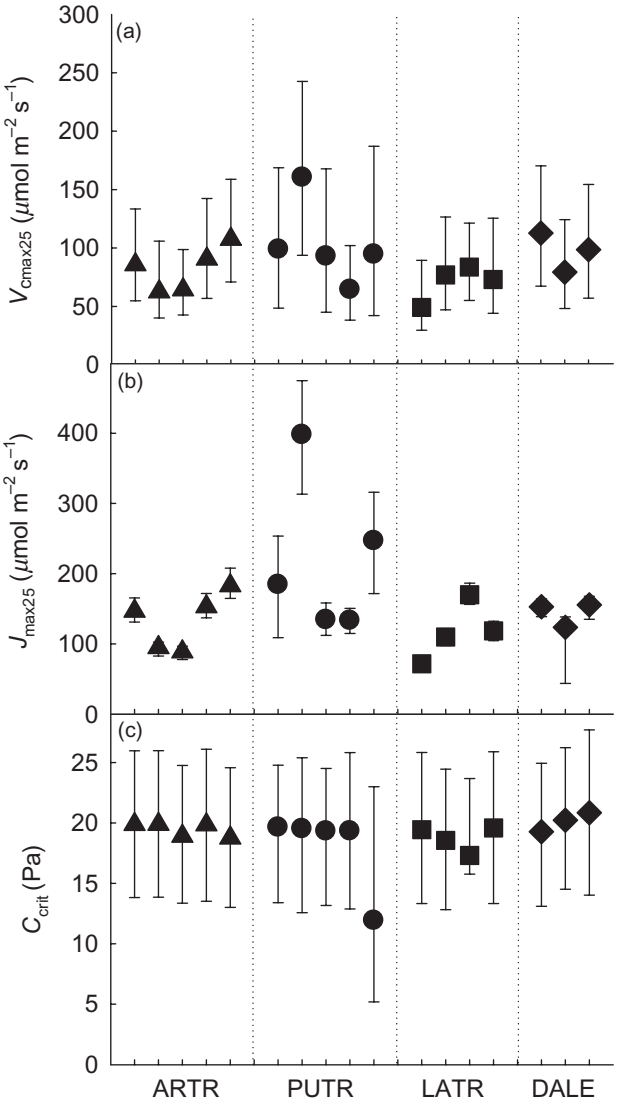

Figure 2. Posterior mean estimates and 95% credible intervals for the plant-level values (i.e. Y_{25p} in Eqn 2) given by the hierarchical Bayesian (HB) model that incorporated A–C_i data only and that implemented the peaked temperature response functions. Estimates are shown for (a) maximum rate of carboxylation standardized to 25 °C (V_{cmax25}), (b) maximum rate of electron transport standardized to 25 °C (J_{max25}) and (c) plant-level transition intercellular partial pressure of CO_2 (C_{crit}). Plant-level estimates are grouped by species where ARTR = *Artemisia tridentata*, PUTR = *Purshia tridentata*, LATR = *Larrea tridentata* and DALE = *Dasylirion leiophyllum*. Symbols correspond to species where ▲ = *A. tridentata*, ● = *P. tridentata*, ■ = *L. tridentata*, ◆ = *D. leiophyllum*. Plants are considered different if the posterior mean for one plant is not contained in the 95% CI for another plant.

RuBP-limited rates) that were well informed by the data, regardless of the data set used. These C_{crit} posterior means ranged from 11.9 to 22.1 Pa across all curves analysed (Fig. 2; Supporting Information Fig. S2). On a plant level, the HB model estimates of g_{m25}, R_{d25}, V_{cmax25} and J_{max25} were also well informed by the photosynthetic data (Figs 1–3). This was demonstrated by narrow credible intervals, posterior means that were quite different from the corresponding prior means, and species differences for some of the parameters (R_{d25}, J_{max25}; Fig. 4). Moreover, many studies have observed a strong, linear correlation between V_{cmax25} and J_{max25} (i.e. J_{max25} tends to be two times V_{cmax25}) (Wullschleger 1993; Leuning 1997; Medlyn *et al.* 2002; Kattge & Knorr 2007). We did not impose any restrictions on the relationship between V_{cmax25} and J_{max25} in our HB model, and we used the model results to evaluate the relationship between these two parameters. The average ratio between the posterior means for plant-level J_{max25} and V_{cmax25} was estimated to be 1.74 ± 0.37 across all species, and V_{cmax25} and J_{max25} were strongly correlated when using A–C_i data only (Fig. 5). This correlation, however, becomes weaker upon incorporation of the A–Q data.

The potential for photosynthetic data to inform model parameters, which are not typically allowed to vary on a

Table 4. Classification of posterior estimates for parameters in the photosynthetic model obtained from the hierarchical Bayesian (HB) analysis using both A–C_i and A–Q data, and peaked temperature functions

Parameter	Well informed	Poorly informed	Species-level differences	Plant-level differences
K_{c25}	×		×	n/a
K_{o25}		×		n/a
Γ^*_{25}	×*			n/a
R_{d25}	×		×	×
V_{cmax25}	×			×
J_{max25}	×		×	×
E_{kc}		×		n/a
E_{ko}		×		n/a
E_g		×		n/a
E_m		×		n/a
E_r		×		n/a
E_v		×		n/a
E_j		×		n/a
g_m	×			×
ΔS_{gm}	×*			n/a
H_{gm}		×		n/a
ΔS_v	×		×	n/a
H_v		×		n/a
ΔS_j	×		×	n/a
H_j		×		n/a

Posterior means and credible intervals (CIs) were evaluated and compared to the prior means and CIs to determine the degree to which parameter estimates were informed by the photosynthetic data. Estimated parameters were classified as well informed by observed data if the posterior means were different from the prior means, had narrow CIs and/or exhibited plant- or species-level variation. Estimated parameters were poorly informed if the posterior estimates were similar to the prior means and had wide CIs. Parameter estimates were also evaluated to determine if they differed between species. An × in a cell indicates how a parameter was classified; an asterisk (*) indicates the parameter was constrained by an informative prior distribution and may become well informed if the priors are relaxed. (For example, although the prior was informative, the posterior mean estimate was different from the prior mean on a plant or species level.)

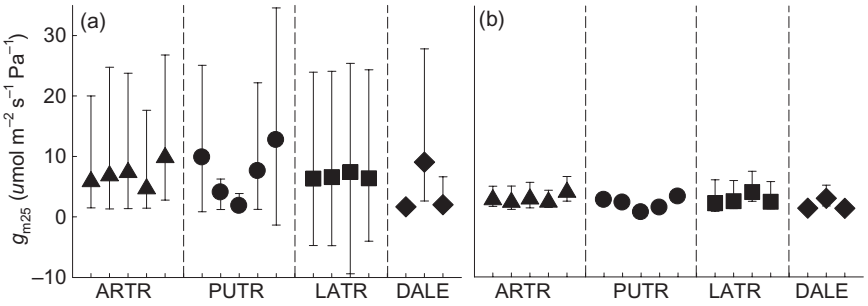

Figure 3. Posterior mean estimates and 95% credible intervals for the plant-level values for mesophyll conductance standardized to 25 °C (g_{m25}) given by the hierarchical Bayesian (HB) model that incorporated A–C_i data only and that implemented the (a) peaked and (b) non-peaked temperature response functions for the four study species (see Fig. 2 for species abbreviations and symbol codes). Plants are considered different if the posterior mean for one plant is not contained in the 95% CI for another plant.

plant and species level, was demonstrated by significant species differences in posterior mean estimates (K_{c25}, ΔS_v and ΔS_j) and variability in the width of their credible intervals (Fig. 4; Supporting Information Fig. S3). Species-level estimates of Γ^*_{25} and ΔS_{gm} were constrained by informative prior distributions, but may become well informed if the priors are relaxed. For example, species-level posterior mean estimates of Γ^*_{25} ranged from 4.7 to 5.9 Pa (Supporting Information Fig. S3), which is greater than the value currently used in most photosynthetic models (3.86 Pa, von Caemmerer *et al.* 1994). While the posterior credible intervals for the two species-level estimates of Γ^*_{25} did contain the prior mean value of 3.86 Pa, estimates for the other two species were significantly different, thus supporting the potential for this parameter to become well informed with relaxed priors. Interestingly, plant-level model estimates of g_{m25} using the non-peaked temperature functions had narrower credible intervals than model estimates of g_{m25} using the peaked temperature functions (Fig. 3). All results are summarized in Table 4.

DISCUSSION

We used an HB framework to couple the Farquhar *et al.* model with photosynthetic data to estimate plant- and/or species-level variability in kinetic constants, biochemical and photosynthetic parameters. The HB approach was successful in that it explicitly estimated the uncertainty or variability in the photosynthetic parameters, many of which are often held constant in applications of the Farquhar *et al.*

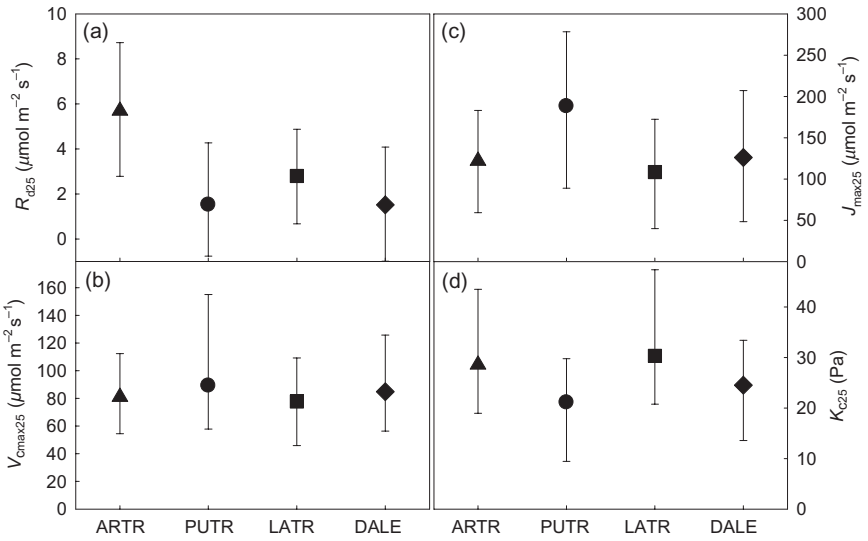

Figure 4. Posterior mean estimates and 95% credible intervals for the species-level values (i.e. μY_{25s} in Eqn 8) given by the hierarchical Bayesian (HB) model that implemented the peaked temperature response function and that incorporated both A–C_i and A–Q data for (a) mitochondrial respiration standardized to 25 °C (R_{d25}), and only A–C_i data for (b) maximum rate of carboxylation standardized to 25 °C (V_{cmax25}), (c) maximum rate of electron transport standardized to 25 °C (J_{max25}) and (d) Michaelis–Menten constant of ribulose 1·5-bisphosphate carboxylase/oxygenase (Rubisco) for CO_2 standardized to 25 °C (K_{c25}) for the four study species (see Fig. 2 for species abbreviations and symbol codes). Species are considered different if the posterior mean for one species is not contained in the 95% CI for another species.

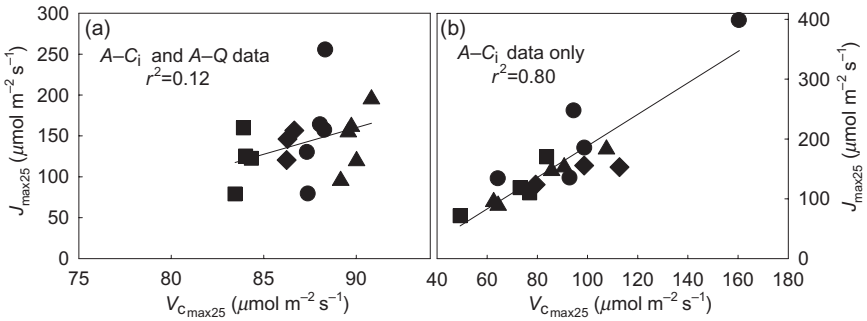

Figure 5. The relationship between plant-level posterior mean estimates for V_{cmax25} (maximum rate of carboxylation) and J_{max25} (maximum rate of electron transport) standardized to 25 °C. That is, the points are the posterior means for plant-specific values of V_{cmax25} and J_{max25} based on the hierarchical Bayesian (HB) model that incorporated peaked Arrhenius temperature functions and used either (a) A–C_i data only or (b) A–C_i and A–Q data combined. Symbols correspond to species where ▲ = *Artemisia tridentata*, ● = *Purshia tridentata*, ■ = *Larrea tridentata*, ◆ = *Dasylirion leiophyllum*.

model. For example, variability in parameters associated with temperature dependence (e.g. E) and Rubisco properties (e.g. K_{c25}) was accounted for and estimated in the HB model (see Supporting Information Table S2), in addition to estimating parameters more directly linked with photosynthesis (g_m, R_d, V_{cmax}, J_{max}).

These parameters could be estimated via the rigorous HB statistical approach that accommodated multiple types of response curve data and that incorporated simultaneous plant-level estimates of C_{crit}. C_{crit} is a critical parameter in the model because it dictates the value of C_i used to differentiate between Rubisco and RuBP limitations. Usually, C_{crit} values are manually set at approximately 20–25 Pa based on work with *Phaesolus vulgaris* (von Caemmerer & Farquhar 1981; Wullschleger 1993; Wohlfahrt *et al.* 1999b; Bunce 2000), but this relatively ad hoc approach to fitting the Farquhar *et al.* model to gas exchange data and the assumption of a fixed transition value across species has been contested (Ethier & Livingston 2004; Dubois *et al.* 2007). The need for a plant- and/or species-specific C_{crit} value has been supported by recent studies on trees (e.g. Douglas fir trees, Ethier & Livingston 2004), and was even demonstrated by early studies that transformed relationships between photosynthesis and chloroplastic CO_2 (Cc) into rates of RuBP regeneration or actual rates of electron transport, and then plotted these values against Cc to determine C_{crit} (von Caemmerer & Farquhar 1981; Kirschbaum & Farquhar 1984). The HB approach described herein provides a feasible method for estimating this key parameter.

In addition to our statistical fitting approach, this study is unique in its simultaneous use of both A–C_i and A–Q curve data to inform estimates of photosynthetic parameters. With the inclusion of A–Q data, estimates of R_{d25} were positive and therefore more biologically realistic. Other studies that fit the Farquhar *et al.* model to A–C_i data have had difficulty in obtaining accurate or biologically realistic estimates of R_{d25} (but see Dubois *et al.* 2007), and as such, R_{d25} is sometimes not reported (Medlyn *et al.* 2002). Additionally, when using the combined data set, species differences in R_{d25} were observed where *A. tridentata* had a significantly greater R_{d25} (5.7 μmol m^{-2} s^{-1}) than the other three species (1.5–2.8 μmol m^{-2} s^{-1}). Although knowledge about the regulation of R_d is generally limited (Nunes-Nesi, Sweetlove & Fernie 2007), recent work using isotopic techniques has shown that R_d plays a role in sustaining photorespiratory nitrogen cycling and perhaps nitrate assimilation (Tcherkez *et al.* 2008). This implies that *A. tridentata* may differ in nitrogen-use efficiency or ATP requirements for the sucrose synthesis and tricarboxylic acid (TCA) cycle intermediates compared to other desert species (Tcherkez *et al.* 2008). Furthermore, in some photosynthetic models, R_d is modelled as a function of V_{cmax}, where R_d set at 0.01–0.02 times V_{cmax} (von Caemmerer 2000); this relationship has been invoked to account for correlations between R_d and leaf nitrogen. At similar temperatures, the posterior means for R_{d25} were on average 0.03 times V_{cmax25} and were within the range of reported literature values from *in vivo* measurements (Bernacchi *et al.* 2001; Warren & Dreyer 2006). By assimilating both A–C_i and A–Q data, the HB approach estimated this 'difficult' parameter on both a species and plant level, and the estimates were consistent with values reported in the literature based on direct measurements of R_d (Bernacchi *et al.* 2001; Warren & Dreyer 2006).

The type of temperature response function needed to accurately fit the Farquhar *et al.* model to photosynthetic data is often species dependent (e.g. Medlyn *et al.* 2002). Subsequently, we compared model fit between the standard, exponential Arrhenius function (Eqn 2) and the peaked exponential function (Eqn 5), and model goodness-of-fit improved with the peaked function model. Some studies suggest that the peaked function is over-parameterized, thereby increasing the difficulty in estimating photosynthetic parameters (Harley *et al.* 1992; Dreyer *et al.* 2001; June, Evans & Farquhar 2004). Conversely, we found that the peaked function was best suited for our native desert plants, which are often exposed to hot and highly variable temperatures. However, it should be noted that posterior mean estimates of g_{m25} had tighter credible intervals and more plant-level variability using the non-peaked model compared to the peaked model. Poor estimates of g_m using the

peaked model may be caused by incorporating prior knowledge of g_m temperature dependencies based on plants from mesic ecosystems. While estimates of g_m for C_3 herbaceous annuals and woody perennials in mesic ecosystems have been shown to be affected by environmental conditions such as soil water deficit (Flexas *et al.* 2002, 2009; Galle *et al.* 2009; Perez-Martin *et al.* 2009), few studies report how temperature affects g_m in desert species. Further study of the effect of environmental variation on g_m in desert plants is needed to correctly parameterize temperature dependency functions for these species.

Utilization of peaked temperature functions was further supported in that species differences were observed for estimates of the temperature function parameters ΔS_v (with the inclusion of A–Q data) and ΔS_j (using A–C_i data only; Supporting Information Fig. S3). Interestingly, both ΔS_v and ΔS_j were given informative prior distributions (Supporting Information Table S1), but the data resulted in posteriors that differed from the priors and that varied among species. To explore the implications of these differences for species-specific temperature responses, we recognize that the optimum temperature for V_{cmax} and J_{max} (T_{opt}) is inversely proportional to ΔS (Medlyn *et al.* 2002; Kattge & Knorr 2007). For example, *P. tridentata* in the Great Basin Desert had greater values for ΔS_v (lower T_{optv}) than plants in the Mojave Desert (*L. tridentata*) and Chihuahuan Desert (*D. leiophyllym*). *P. tridentata* had significantly greater values for ΔS_j (lower T_{optj}) than all other species. Further, these differences in T_{opt} may reflect differences in plant growth temperatures (Hikosaka, Murakami & Hirose 1999; Medlyn *et al.* 2002; Bernacchi, Pimentel & Long 2003; Onoda, Hikosaka & Hirose 2005). Because the Great Basin Desert is a cold desert, and the Mojave and Chihuahuan Deserts are hot deserts, the optimum temperature for maximum carbon assimilation in our study species may be related to growing season temperature. Indeed, in an analysis of 36 species, Kattge & Knorr (2007) found that plant growth temperature did not significantly affect V_{cmax} at a given base rate temperature, but did affect T_{opt} for V_{cmax}.

Species differences were also observed for model estimates of K_{c25} and J_{max25}. Because K_{c25} was assigned an informative prior distribution based on literature data that were the same for all species (Supporting Information Table S1), the photosynthetic curve data, and not the prior distribution, were the primary determinants of the posterior estimates of K_{c25}. Few modelling studies have estimated Michaelis–Menten parameters (K_{c25}, K_{o25}) because of the difficulty in collecting field data directly related to these parameters (but see von Caemmerer 2000; Ethier & Livingston 2004); interestingly, observed data influenced the posterior distributions for K_{c25} in this study. While this parameter describes intrinsic properties of Rubisco and is generally assumed constant across species (von Caemmerer 2000), our results show that K_{c25} should not be held constant across plants, species and functional types when estimating V_{cmax} and J_{max}. Importantly, we did not assume constant values for the kinetic constants or the temperature response parameters, but rather used informative priors to account for variability, thereby obtaining more accurate estimates for parameters directly related to V_{cmax} and J_{max}.

Posterior estimates of species-level J_{max25} showed that it was significantly greater in *P. tridentata* compared to *A. tridentata* and *L. tridentata*. Given that J_{max25} may be influenced by environmental conditions (e.g. light, soil moisture), these results suggest that *P. tridentata* may have comparatively greater access to resources compared to the other species. This is partially supported by the observation that *P. tridentata* has a bimodal rooting distribution (Loik 2007), and thus it may utilize both stable (deep) and ephemeral (near-surface) water sources. Its surface roots may also facilitate uptake of nutrients from shallow soil layers. Greater access to water and nutrients is expected to increase the efficiency of electron transport. Because species have varying strategies for adapting to different environments, we suggest that photosynthesis should be measured under a wide range of environmental conditions (e.g. rooting depth, high-temperature stress, nutrient limitation, low soil moisture) and subsequently analysed using the flexible HB approach described herein. Using this approach, one can explicitly acknowledge important sources of uncertainty and accommodate variation in environmental drivers, existing knowledge about the photosynthetic process and parameters and diverse data sets to obtain more accurate estimates of species-level photosynthetic parameters (e.g. V_{cmax25}, J_{max25}).

In addition to accounting for species-level variability, results from our HB fitting approach highlight the importance of recognizing plant-level variability when estimating photosynthetic parameters using the Farquhar *et al.* model. Significant plant-level variation was observed for g_m, R_d, V_{cmax25} and J_{max25} (Figs 1–3). Because there was greater plant-level variation observed than species-level variation, this highlights the potential importance of small-scale variation in environmental variables for understanding photosynthetic responses in desert plants. Indeed, it has been well documented that V_{cmax25} exhibits high variation as a function of species identity, nutrient availability, season, leaf age and leaf position within the canopy (Medlyn *et al.* 1999; Wilson, Baldocchi & Hanson 2000; Misson *et al.* 2006). This study also indicates that plant-level variation must be accounted for when obtaining estimates of species-level photosynthetic parameters. Otherwise, if variability among plants is ignored, then the species-level parameter estimates and their associated uncertainties will be compromised.

CONCLUSIONS

The HB approach presented herein allowed us to rigorously fit fairly complicated photosynthetic models to fairly simple data sets via a probabilistic modelling approach that: (1) simultaneously analysed diverse data sources (both A–C_i and A–Q curves) that informed the same underlying physiological processes; (2) explicitly accounted for and estimated parameter uncertainty for desert plant species, thereby filling a gap in our understanding of plant photosynthetic responses as most empirical studies have focused

on mesic temperate species; (3) avoided ad hoc model tuning by incorporating informative prior information derived from the literature to help constrain parameters that are not well informed by the field data (e.g. activation energies); and (4) did not require fixed parameter specifications, but rather was able to accommodate different degrees of model flexibility and prior information, allowing for a rigorous evaluation of photosynthetic parameters and different sources of variability. As such, the HB model of C_3 photosynthesis successfully predicted observed photosynthesis. In addition, it yielded explicit plant-level estimates for C_{crit}, and plant- and species-level estimates for photosynthetic parameters (g_{m25}, R_{d25}, V_{cmax25} and J_{max25}) for desert plants. In summary, the HB approach has great potential to improve the estimation of photosynthetic parameters across a wide range of C_3 species, thereby extending the applicability and utility of process-based models such as the Farquhar *et al.* model. The ease of implementation and flexibility of the HB modelling approach make this an important tool that may be applied to a variety of ecosystems and experimental design settings.

ACKNOWLEDGMENTS

We thank Travis Huxman, Michael Loik and Stan Smith for access to their study sites and use of their equipment. Assistance in the field and logistical support were provided by Holly Alpert, Greg Barron-Gafford, Topher Bentley, Jessie Cable, Dene Charlet, Dan Dawson, Earthwatch Mammoth Lakes SCAP students, Allison Ebbets, Alex Eilts, Lynn Fenstermaker, Alden Griffith, Danielle Ignace, Traesha Robertson, Joe Sirotnak, Anna Tyler and Natasja van Gestel. Victor Resco de Dios, Graham Farquhar and two anonymous reviewers provided valuable comments on earlier drafts of this manuscript. The research described in this paper has been funded in part by the United States Environmental Protection Agency (EPA) under the Greater Research Opportunities (GRO) Graduate Program (L.D.P.). EPA has not officially endorsed this publication, and the views expressed herein may not reflect the views of the EPA. This study was also supported by a US National Park Service grant (D.T.T.) and a US Department of Energy NICCR grant (K.O., D.T.T.).

REFERENCES

Baldocchi D.D. & Harley P.C. (1995) Scaling carbon-dioxide and water-vapor exchange from leaf to canopy in a deciduous forest. 2. Model testing and application. *Plant, Cell & Environment* **18,** 1157–1173.

Barker D.H., Vanier C., Naumburg E., Charlet T.N., Nielsen K.M., Newingham B.A. & Smith S.D. (2006) Enhanced monsoon precipitation and nitrogen deposition affect leaf traits and photosynthesis differently in spring and summer in the desert shrub *Larrea tridentata*. *New Phytologist* **169,** 799–808.

Bernacchi C.J., Singsaas E.L., Pimentel C., Portis A.R. & Long S.P. (2001) Improved temperature response functions for models of Rubisco-limited photosynthesis. *Plant, Cell & Environment* **24,** 253–259.

Bernacchi C.J., Pimentel C. & Long S.P. (2003) *In vivo* temperature response functions of parameters required to model RuBP-limited photosynthesis. *Plant, Cell & Environment* **26,** 1419–1430.

Bjorkman O., Badger M.R. & Armond P.A. (1980) Response and adaptation of photosynthesis at high temperature. In *Adaptation of Plants to Water and High Temperature Stress* (eds N.C. Turner & P.J. Kramer), pp. 233–249. John Wiley & Sons, New York, NY, USA.

Brooks S.P. & Gelman A. (1998) General methods for monitoring convergence of iterative simulations. *Journal of Computational and Graphical Statistics* **7,** 434–455.

Bunce J.A. (2000) Acclimation of photosynthesis to temperature in eight cool and warm climate herbaceous C-3 species: temperature dependence of parameters of a biochemical photosynthesis model. *Photosynthesis Research* **63,** 59–67.

Cable J.M., Ogle K., Williams D.G., Weltzin J. & Huxman T.E. (2008) Soil texture drives responses of soil respiration to precipitation pulses in the Sonoran Desert: implications for climate change. *Ecosystems* **11,** 961–979.

Cable J.M., Ogle K., Tyler A.P., Pavao-Zuckerman M.A. & Huxman T.E. (2009) Woody plant encroachment impacts on soil carbon and microbial processes: results from a hierarchical Bayesian analysis of soil incubation data. *Plant and Soil* **320,** 153–167.

von Caemmerer S. (2000) *Biochemical Models of Leaf Photosynthesis*. CSIRO, Collingswood, NJ, USA.

von Caemmerer S. & Evans J.R. (1991) Determination of the average partial-pressure of CO_2 in chloroplasts from leaves of several C_3 plants. *Australian Journal of Plant Physiology* **18,** 287–305.

von Caemmerer S. & Farquhar G.D. (1981) Some relationships between the biochemistry of photosynthesis and the gas exchange of leaves. *Planta* **153,** 376–387.

von Caemmerer S., Evans J.R., Hudson G.S. & Andrews T.J. (1994) The kinetics of ribulose-1,5-bisphosphate carboxylase/oxygenase *in-vivo* inferred from measurements of photosynthesis in leaves of transgenic tobacco. *Planta* **195,** 88–97.

Carlin B.P., Clark J.S. & Gelfand A.E. (2006) Elements of hierarchical Bayesian inference. In *Hierarchical Modelling for the Environmental Sciences: Statistical Methods and Applications* (eds J.S. Clark & A.E. Gelfand), pp. 3–24. Oxford University Press, New York, NY, USA.

Clark J.S. (2005) Why environmental scientists are becoming Bayesians. *Ecology Letters* **8,** 2–14.

Clark J.S. & Gelfand A.E. (2006) *Hierarchical Modelling for the Environmental Sciences*. Oxford University Press, Oxford, UK.

Clark J. & LaDeau S. (2006) Synthesizing ecological experiments and observational data with hierarchical Bayes. In *Hierarchical Modelling for the Environmental Sciences* (eds J.S. Clark & A.E. Gelfand), pp. 41–58. Oxford University Press, Oxford, UK.

Dreyer E., Le Roux X., Montpied P., Daudet F.A. & Masson F. (2001) Temperature response of leaf photosynthetic capacity in seedlings from seven temperate tree species. *Tree Physiology* **21,** 223–232.

Dubois J.J.B., Fiscus E.L., Booker F.L., Flowers M.D. & Reid C.D. (2007) Optimizing the statistical estimation of the parameters of the Farquhar–von Caemmerer–Berry model of photosynthesis. *New Phytologist* **176,** 402–414.

Ethier G.J. & Livingston N.J. (2004) On the need to incorporate sensitivity to CO_2 transfer conductance into the Farquhar–von Caemmerer–Berry leaf photosynthesis model. *Plant, Cell & Environment* **27,** 137–153.

Evans J.R. (1987) The dependence of quantum yield on wavelength and growth irradiance. *Australian Journal of Plant Physiology* **14,** 69–79.

Evans J.R. (1989) Photosynthesis and nitrogen relationships in leaves of C-3 plants. *Oecologia* **78,** 9–19.

Evans J.R. & von Caemmerer S. (1996) Carbon dioxide diffusion inside leaves. *Plant Physiology* **110,** 339–346.

Farquhar G.D. & Wong S.C. (1984) An empirical model of stomatal conductance. *Australian Journal of Plant Physiology* **11,** 191–210.

Farquhar G.D., von Caemmerer S. & Berry J.A. (1980) A biochemical-model of photosynthetic CO_2 assimilation in leaves of C-3 species. *Planta* **149,** 78–90.

Flexas J., Bota J., Escalona J.M., Sampol B. & Medrano H. (2002) Effects of drought on photosynthesis in grapevines under field conditions: an evaluation of stomatal and mesophyll limitations. *Functional Plant Biology* **29,** 461–471.

Flexas J., Baron M., Bota J., *et al.* (2009) Photosynthesis limitations during water stress acclimation and recovery in the drought-adapted *Vitis* hybrid Richter-110 (*V. berlandieri* × *V. rupestris*). *Journal of Experimental Botany* **60,** 2361–2377.

Foley J.A., Levis S., Prentice I.C., Pollard D. & Thompson S.L. (1998) Coupling dynamic models of climate and vegetation. *Global Change Biology* **4,** 561–579.

Galle A., Florez-Sarasa I., Tomas M., Pou A., Medrano H., Ribas-Carbo M. & Flexas J. (2009) The role of mesophyll conductance during water stress and recovery in tobacco (*Nicotiana sylvestris*): acclimation or limitation? *Journal of Experimental Botany* **60,** 2379–2390.

Gamerman D. & Hedibert F.L. (2006) *Markov Chain Monte Carlo: Stochastic Simulation for Bayesian Inference*, 2nd edn. Chapman & Hall/CRC, Boca Raton, FL, USA.

Gelfand A.E. & Ghosh S.K. (1998) Model choice: a minimum posterior predictive loss approach. *Biometrika* **85,** 1–11.

Gelman A. (2004a) Exploratory data analysis for complex models. *Journal of Computational and Graphical Statistics* **13,** 755–779.

Gelman A. (2004b) Parameterization and Bayesian modeling. *Journal of the American Statistical Association* **99,** 537–545.

Gelman A. (2006) Prior distributions for variance parameters in hierarchical models. *Bayesian Analysis* **1,** 515–533.

Gelman A., Carlin J.B., Stern H.S. & Rubin D.B. (2004) *Bayesian Data Analysis*, 2nd edn. Chapman & Hall, Boca Raton, FL, USA.

Gillespie I.G. & Loik M.E. (2004) Pulse events in Great Basin Desert shrublands: physiological responses of *Artemisia tridentata* and *Purshia tridentata* seedlings to increased summer precipitation. *Journal of Arid Environments* **59,** 41–57.

Harley P.C., Thomas R.B., Reynolds J.F. & Strain B.R. (1992) Modeling photosynthesis of cotton grown in elevated CO_2. *Plant, Cell & Environment* **15,** 271–282.

Hikosaka K., Murakami A. & Hirose T. (1999) Balancing carboxylation and regeneration of ribulose-1,5-bisphosphate in leaf photosynthesis: temperature acclimation of an evergreen tree, *Quercus myrsinaefolia*. *Plant, Cell & Environment* **22,** 841–849.

Hunter R.B. (compiler, 1995) *Status of the Flora and Fauna on the Nevada Test Site, 1994*, DOE/NV 11432-195. Reynolds Electrical & Engineering Co., Inc., Las Vegas, NV, USA.

Johnson F.H., Eyring H. & Williams R.W. (1942) The nature of enzyme inhibitions in bacterial luminescence – sulfanilamide, urethane, temperature and pressure. *Journal of Cellular and Comparative Physiology* **20,** 247–268.

June T., Evans J.R. & Farquhar G.D. (2004) A simple new equation for the reversible temperature dependence of photosynthetic electron transport: a study on soybean leaf. *Functional Plant Biology* **31,** 275–283.

Kattge J. & Knorr W. (2007) Temperature acclimation in a biochemical model of photosynthesis: a reanalysis of data from 36 species. *Plant, Cell & Environment* **30,** 1176–1190.

Kimball J.S., Keyser A.R., Running S.W. & Saatchi S.S. (2000) Regional assessment of boreal forest productivity using an ecological process model and remote sensing parameter maps. *Tree Physiology* **20,** 761–775.

Kirschbaum M.U.F. & Farquhar G.D. (1984) Temperature dependence of whole leaf photosynthesis in *Eucalyptus pauciflora*. *Australian Journal of Plant Physiology* **11,** 519–538.

Leuning R. (1997) Scaling to a common temperature improves the correlation between the photosynthesis parameters *J*(max) and *V*-cmax. *Journal of Experimental Botany* **48,** 345–347.

Leuning R. (2002) Temperature dependence of two parameters in a photosynthesis model. *Plant, Cell & Environment* **25,** 1205–1210.

Lloyd J., Syvertsen J.P., Kriedemann P.E. & Farquhar G.D. (1992) Low conductances for CO_2 diffusion from stomata to the sites of carboxylation in leaves of woody species. *Plant, Cell & Environment* **15,** 873–899.

Loik M.E. (2007) Sensitivity of water relations and photosynthesis to summer precipitation pulses for *Artemesia tridentata* and *Purshia tridentata*. *Plant Ecology* **191,** 95–108.

Loreto F., Harley P.C., Dimarco G. & Sharkey T.D. (1992) Estimation of mesophyll conductance to CO_2 flux by 3 different methods. *Plant Physiology* **98,** 1437–1443.

Loreto F., Tsonev T. & Centritto M. (2009) The impact of blue light on leaf mesophyll conductance. *Journal of Experimental Botany* **60,** 2283–2290.

Lunn D.J., Thomas A., Best N. & Spiegelhalter D. (2000) WinBUGS – a Bayesian modelling framework: concepts, structure, and extensibility. *Statistics and Computing* **10,** 325–337.

Manter D.K. & Kerrigan J. (2004) *A*/*C*-i curve analysis across a range of woody plant species: influence of regression analysis parameters and mesophyll conductance. *Journal of Experimental Botany* **55,** 2581–2588.

Medlyn B.E., Badeck F.W., De Pury D.G.G., *et al.* (1999) Effects of elevated [CO_2] on photosynthesis in European forest species: a meta-analysis of model parameters. *Plant, Cell & Environment* **22,** 1475–1495.

Medlyn B.E., Loustau D. & Delzon S. (2002) Temperature response of parameters of a biochemically based model of photosynthesis. I. Seasonal changes in mature maritime pine (*Pinus pinaster* Ait.). *Plant, Cell & Environment* **25,** 1155–1165.

Miao Z.W., Xu M., Lathrop R.G. & Wang Y.F. (2009) Comparison of the *A*-*C*-c curve fitting methods in determining maximum ribulose 1.5-bisphosphate carboxylase/oxygenase carboxylation rate, potential light saturated electron transport rate and leaf dark respiration. *Plant, Cell & Environment* **32,** 109–122.

Misson L., Tu K.P., Boniello R.A. & Goldstein A.H. (2006) Seasonality of photosynthetic parameters in a multi-specific and vertically complex forest ecosystem in the Sierra Nevada of California. *Tree Physiology* **26,** 729–741.

Niinemets O., Diaz-Espejo A., Flexas J., Galmes J. & Warren C.R. (2009a) Importance of mesophyll diffusion conductance in estimation of plant photosynthesis in the field. *Journal of Experimental Botany* **60,** 2271–2282.

Niinemets O., Diaz-Espejo A., Flexas J., Galmes J. & Warren C.R. (2009b) Role of mesophyll diffusion conductance in constraining potential photosynthetic productivity in the field. *Journal of Experimental Botany* **60,** 2249–2270.

Nunes-Nesi A., Sweetlove L.J. & Fernie A.R. (2007) Operation and function of the tricarboxylic acid cycle in the illuminated leaf. *Physiologia Plantarum* **129,** 45–56.

Ogle K. & Barber J.J. (2008) Bayesian data-model integration in plant physiological and ecosystem ecology. *Progress in Botany* **69,** 281–311.

Ogle K. & Reynolds J.F. (2002) Desert dogma revisited: coupling of stomatal conductance and photosynthesis in the desert shrub, *Larrea tridentata*. *Plant, Cell & Environment* **25,** 909–921.

Ogle K., Barber J.J., Willson C.J. & Thompson B. (2009) Hierarchical statistical modeling of xylem vulnerability to cavitation. *New Phytologist* **182,** 541–554.

Onoda Y., Hikosaka K. & Hirose T. (2005) The balance between RuBP carboxylation and RuBP regeneration: a mechanism underlying the interspecific variation in acclimation of photosynthesis to seasonal change in temperature. *Functional Plant Biology* **32,** 903–910.

Patrick L., Cable J., Potts D., *et al.* (2007) Effects of an increase in summer precipitation on leaf, soil, and ecosystem fluxes of CO_2 and H_2O in a sotol grassland in Big Bend National Park, Texas. *Oecologia* **151,** 704–718.

Patrick L.D., Ogle K., Bell C.W., Zak J. & Tissue D. (2009) Physiological responses of two contrasting desert plant species to precipitation variability are differentially regulated by soil moisture and nitrogen dynamics. *Global Change Biology* **15,** 1214–1229.

Perez-Martin A., Flexas J., Ribas-Carbo M., Bota J., Tomas M., Infante J.M. & Diaz-Espejo A. (2009) Interactive effects of soil water deficit and air vapour pressure deficit on mesophyll conductance to CO_2 in *Vitis vinifera* and *Olea europaea*. *Journal of Experimental Botany* **60,** 2391–2405.

Pitman A.J. (2003) The evolution of, and revolution in, land surface schemes designed for climate models. *International Journal of Climatology* **23,** 479–510.

Pons T.L., Flexas J., von Caemmerer S., Evans J.R., Genty B., Ribas-Carbo M. & Brugnoli E. (2009) Estimating mesophyll conductance to CO_2: methodology, potential errors, and recommendations. *Journal of Experimental Botany* **60,** 2217–2234.

dePury D.G.G. & Farquhar G.D. (1997) Simple scaling of photosynthesis from leaves to canopies without the errors of big-leaf models. *Plant, Cell & Environment* **20,** 537–557.

Robertson T.R., Bell C.W., Zak J.C. & Tissue D.T. (2009) Precipitation timing and magnitude differentially affect aboveground annual net primary productivity in three perennial species in a Chihuahuan Desert grassland. *New Phytologist* **181,** 230–242.

Sellers P.J., Randall D.A., Collatz G.J., Berry J.A., Field C.B., Dazlich D.A., Zhang C., Collelo G.D. & Bounoua L. (1996) A revised land surface parameterization (SiB2) for atmospheric GCMs. 1. Model formulation. *Journal of Climate* **9,** 676–705.

Sharkey T.D., Bernacchi C.J., Farquhar G.D. & Singsaas E.L. (2007) Fitting photosynthetic carbon dioxide response curves for C-3 leaves. *Plant, Cell & Environment* **30,** 1035–1040.

Tcherkez G.G.B., Farquhar G.D. & Andrews T.J. (2006) Despite slow catalysis and confused substrate specificity, all ribulose bisphosphate carboxylases may be nearly perfectly optimized. *Proceedings of the National Academy of Sciences of the United States of America* **103,** 7246–7251.

Tcherkez G., Bligny R., Gout E., Mahe A., Hodges M. & Cornic G. (2008) Respiratory metabolism of illuminated leaves depends on CO_2 and O-2 conditions. *Proceedings of the National Academy of Sciences of the United States of America* **105,** 797–802.

Tholen D., Boom C., Noguchi K., Ueda S., Katase T. & Terashima I. (2008) The chloroplast avoidance response decreases internal conductance to CO_2 diffusion in *Arabidopsis thaliana* leaves. *Plant, Cell & Environment* **31,** 1688–1700.

Warren C.R. (2008) Stand aside stomata, another actor deserves centre stage: the forgotten role of the internal conductance to CO_2 transfer. *Journal of Experimental Botany* **59,** 1475–1487.

Warren C.R. & Dreyer E. (2006) Temperature response of photosynthesis and internal conductance to CO_2: results from two independent approaches. *Journal of Experimental Botany* **57,** 3057–3067.

Wikle C.K. (2003) Hierarchical models in environmental science. *International Statistical Review* **71,** 181–199.

Williams M., Law B.E., Anthoni P.M. & Unsworth M.H. (2001) Use of a simulation model and ecosystem flux data to examine carbon–water interactions in ponderosa pine. *Tree Physiology* **21,** 287–298.

Wilson K.B., Baldocchi D.D. & Hanson P.J. (2000) Spatial and seasonal variability of photosynthetic parameters and their relationship to leaf nitrogen in a deciduous forest. *Tree Physiology* **20,** 565–578.

Wohlfahrt G., Bahn M. & Cernusca A. (1999a) The use of the ratio between the photosynthesis parameters *P*-ml and *V*-cmax for scaling up photosynthesis of C-3 plants from leaves to canopies: a critical examination of different modelling approaches. *Journal of Theoretical Biology* **200,** 163–181.

Wohlfahrt G., Bahn M., Haubner E., Horak I., Michaeler W., Rottmar K., Tappeiner U. & Cernusca A. (1999b) Inter-specific variation of the biochemical limitation to photosynthesis and related leaf traits of 30 species from mountain grassland ecosystems under different land use. *Plant, Cell & Environment* **22,** 1281–1296.

Wullschleger S.D. (1993) Biochemical limitations to carbon assimilation in C(3) plants – a retrospective analysis of the *A*/*C*i curves from 109 species. *Journal of Experimental Botany* **44,** 907–920.

Received 5 June 2009; received in revised form 13 July 2009; accepted for publication 14 July 2009

SUPPORTING INFORMATION

Additional Supporting Information may be found in the online version of this article:

Figure S1. Examples of typical gas exchange data collected from (a) a CO_2 response curve (A–C_i) and (b) a light response curve (A–Q).

Figure S2. Posterior mean estimates and 95% credible intervals for the plant-level values (i.e. Y_{25p} in Eqn 7) using the HB model with both A–C_i and A–Q data, and peaked temperature response functions for (a) maximum rate of carboxylation standardized to 25 °C (V_{cmax25}), (b) maximum rate of electron transport standardized to 25 °C (J_{max25}) and (c) plant-level transition intercellular partial pressure of CO_2 (C_{crit}). Plant-level estimates are grouped by species where ARTR = *Artemisia tridentata*, PUTR = *Purshia tridentata*, LATR = *Larrea tridentata* and DALE = *Dasylirion leiophyllum*. Symbols correspond to species where ▲ = *A. tridentata*, ● = *P. tridentata*, ■ = *L. tridentata*, ◆ = *D. leiophyllum*.

Figure S3. Posterior mean estimates and 95% credible intervals for the species-level values of the entropy factor used in Arrhenius temperature function (ΔS) for (a) g_{m25} (using A–C_i data only), (b) V_{cmax25} (using A–C_i and A–Q data), (c) J_{max25} (using A–C_i data only), as well as (d) the CO_2 compensation point in the absence of day respiration (Γ^*_{25}; using A–C_i data only) for the four study species using the hierarchical Bayesian (HB) model with peaked temperature functions (see Fig. S2 for species abbreviations and symbol codes).

Table S1. Median and 95% empirical quantiles for photosynthetic parameter values derived from the literature, with references provided; n/a indicates that information was not available in the literature. Refer to Table 1 for units.

Table S2. Posterior mean and 95% credible interval (CI) estimates for Michaelis–Menten parameters standardized to 25 °C (K_{c25}, K_{o25}), CO_2 compensation point in the absence of day respiration (Γ^*_{25}), activation energies (Es) and peaked Arrhenius temperature variables (Hs, ΔSs), given by the hierarchical Bayesian (HB) model for all four desert shrub species, using A–C_i data only. Posterior 95% CIs that do not contain the posterior mean of another species's parameter indicate significant differences between the two parameter estimates; that is, there is at most a 5% chance that the species have similar parameter values. Refer to Table 1 for units.

Please note: Wiley-Blackwell are not responsible for the content or functionality of any supporting materials supplied by the authors. Any queries (other than missing material) should be directed to the corresponding author for the article.